Canadian Journal of Microbiology

OPEN ACCESS | Article

# *Prototaxites* reinterpreted as mega-rhizomorphs, facilitating nutrient transport in early terrestrial ecosystems

**Vivi Vajda, Larissa Cavalcante, Kristoffer Palmgren, Ashley Krüger, and Magnus Ivarsson**

Department of Palaeobiology, Swedish Museum of Natural History, SE 104 05 Stockholm, Sweden

Corresponding authors: **Vivi Vajda** (email: vivi.vajda@nrm.se); **Magnus Ivarsson** (email: magnus.ivarsson@nrm.se)

Can. J. Microbiol. Downloaded from cdnsciencepub.com by 90.190.215.226 on 05/14/24

## Abstract

The enigmatic fossil *Prototaxites* found in successions ranging from the Middle Ordovician to the Upper Devonian was originally described as having conifer affinity. The current debate, however, suggests that they probably represent gigantic algal–fungal symbioses. Our re-investigation of permineralized *Prototaxites* specimens from two localities, the Heider quarry in Germany and the Bordeaux quarry in Canada, reveals striking anatomical similarities with modern fungal rhizomorphs *Armillaria mellea*. We analysed extant fungal rhizomorphs and fossil *Prototaxites* through light microscopy of their anatomy, Fourier transform infrared spectroscopy, X-ray microscopy, and Raman spectroscopy. Based on these comparisons, we interpret the *Prototaxites* as fungi. The detailed preservation of cell walls and possible organelles seen in transverse sections of *Prototaxites* reveal that fossilization initiated while the organism was alive, inhibiting the collapse of delicate cellular structures. *Prototaxites* has been interpreted to grow vertically by many previous workers. Here we propose an alternative view that *Prototaxites* represents a complex hyphal aggregation (rhizomorph) that may have grown horizontally similar to modern complex aggregated mycelial growth forms, such as cords and rhizomorphs. Their main function was possibly to redistribute water and nutrition from nutrient-rich to nutrient-poor areas facilitating the expansion for early land plant communities.

**Key words:** *Prototaxites*, Devonian, fungus, algae, lichen, hot-spring deposit

## Introduction

The evolution of land plants and their colonization of terrestrial environments are among the fundamental topics within the field of geobiology (Edwards et al. 2014). The rise of plants can be traced via fossil spores preserved in the geological record by these early terrestrial plants. Although traces of early land plants have been recorded from successions as old as the Ordovician (Rubinstein et al. 2011; Badawy et al. 2014; Rubinstein and Vajda 2019; Leslie et al. 2021), a major radiation occurred during the late Silurian and Early Devonian, when plants developed more complex forms, increased in abundance, and became well established on most continents (Gray et al. 1974; Richardson and McGregor 1986; Mehlqvist et al. 2012, 2014, 2015; Wellman et al. 2013, 2022; Leslie et al. 2021). This was also a time when other groups of organisms developed in the terrestrial realm and left behind peculiar fossil remains. One such organism was *Prototaxites loganii* Dawson. This puzzling fossil represents an organism that inhabited the late Silurian to Late Devonian terrestrial landscape (420–370 Ma). It was by far the largest land-living organism at the time, and possibly represented an important carbon source for the early fauna that otherwise only shared the eco-space with minute early land plants and arthropods (Retallack 2001; Hagström and Mehlqvist 2012). Indeed, Hueber (2001) identified the earliest records of terrestrial arthropod borings in a *Prototaxites* "log". The architecture, systematic affinities, and ecology of these organisms have been debated intensely since their initial description by Dawson (1859) who described it under the species name *P. loganii* owing to its superficial resemblance to a conifer trunk. The fossils are remarkably robust, reaching tree size (up to 8 m long and 1 m in diameter), in some cases branching distally, and incorporating concentric layers of longitudinally aligned, smooth, slender tubes interwoven with differentially thickened, banded tubes (Schweitzer 1983). Moreover, many of the fossils show little compaction indicating a rigid architecture of the original organism, or a very rapid process of permineralization.

The suggested affinities of these fossils have, over the past 160 years, included the trunks of vascular plants (Dawson 1859), kelp-like aquatic algae (Schweitzer 1983), or rolled up mats of liverworts (Graham et al. 2010). Hueber (2001) interpreted *Prototaxites* as a giant sporomorph of basidiomycote affinities, whereas Retallack and Landing (2014) favoured a provisional assignment to *Glomeromycota*. Honegger et al. (2018) described *P. loganii* as a giant sporophore (basidioma) and identified fertile *Prototaxites taiti* in Rhynie cherts. Boyce et al. (2007) obtained variable $\delta^{13}C$ isotope values from

Can. J. Microbiol. Downloaded from cdnsciencepub.com by 90.190.215.226 on 05/14/24

*Prototaxites*, suggesting heterotrophic nutrition on isotopically distinct substrates consistent with a fungal affinity. Most recent interpretations have converged on *Prototaxites* being either a fungal fruiting body or large lichen (Selosse 2002; Nelsen and Boyce 2022). In summary, Nematophytales (including *Prototaxites*) have no clear affinities with extant groups but probably constitute a fully extinct array of fungi (Edwards and Axe 2012). Studies of *Prototaxites* have indicated that this organism had a lifestyle adapted to a terrestrial environment, and although an upright growth habit has been proposed for *Prototaxites* by many previous authors, convincing evidence for this is meagre (Graham et al. 2010; Retallack 2022).

Here we explore the morphological and chemical similarities between extant fungal rhizomorphs and *Prototaxites* specimens derived from two Northern Hemisphere localities. We assess the depositional environment of the Early Devonian ecosystem in which these giant organisms lived and discuss their influence on the early land plant communities.

## Materials

### Fossil material

The studied fossil material is represented by two Early Devonian *Prototaxites* associations, one from the Heider quarry (50°57′00″N, 007°18′00″E), Germany, and the other from the Bordeaux quarry (48°02′48″N, 066°46′57″E), Canada. The specimens are part of the paleobotanical collections hosted at the Swedish Museum of Natural History (NRM). The material from the Heider quarry was originally collected by Prof. H.-J. Schweitzer and described in 1983 as *Prototaxites* cf. *loganii* (Dawson). The Heider quarry belongs to the Wahnbach-Schichten of the Rheinische Schiefergebirge (shale mountains) and hosts one of the most important Early Devonian fossil assemblages. The successions are near-shore marine and contain not only a rich fish and eurypterid fauna but also a range of transported early land plant remains (Gross 1933).

The Bordeaux quarry is located on the southern shores of the Gaspé on Chaleur Bay and the river mouth of Restigouche River in Quebec, Canada. The fossils were collected from the Campbellton Formation, which has been dated to an Early Devonian, Emsian age (Kennedy et al. 2013). The assemblage was collected by Dawson in 1881 when visiting the area. The successions represent flood plain deposits intercalated with coarser transported material, in which the *Prototaxites* were found. The Campbellton Formation is overlying the Val d'Amour Formation of Pragian age, which contains abundant volcanoclastic deposits (Kennedy et al. 2013).

### Extant fungal isolates

Three extant fungal isolates T4 (*Armillaria mellea*), T8 (*Postia rennyi*), and T9 (*Fomitopsis pinicola*) of saprophytic fungi from the Tyresta National Reserve, Stockholm, Sweden, sampled in September 2021, were used in the study. The samples were collected from fungal fruiting bodies on tree trunks (Figs. 1A–1C). Within 24 h, the samples were placed in Petri dishes with a growth medium (Sigma–Aldrich's potato glucose agar), and spiked with cloramphenicol (0.05 g $L^{-1}$) at 25 °C. The plates were checked every other day, and when fungal growth was observed, samples were transferred to a new Petri dish and left to incubate. These steps were repeated until isolates were obtained. All three extant fungi were used for Fourier transform infrared (FTIR) analysis for compositional comparison with the fossils and for calculating the $R_{3/2}$ branching index. The *A. mellea* isolate forming morphologically distinct rhizomorphs was used as a morphological comparison to the fossil material (Figs. 1D–1F).

## Methods

### Light and fluorescence microscopy combined with staining

The fungi and fossil samples were studied using a stereomicroscope (Olympus SZX2-ILLT) and an Olympus BX51 microscope with an X-cite Series 120Q fluorescence light source. The fungi were stained with CalcoFlourWhite (BioTium), a dye that binds to chitin. Before staining, the samples were treated with sterile gloves and forceps to reduce the introduction of foreign fluorescent particles.

### ESEM

An XL30 environmental scanning electron microscope (ESEM) with a field emission gun (XL30 ESEM-FEG) was used to analyse the fossil material and the rhizomorphs. The ESEM was equipped with an Oxford x-act energy dispersive spectrometer, a backscatter electron detector, and a secondary electron detector. The acceleration voltage was 20 kV. The instrument was calibrated with a cobalt standard. Peak and element analyses, together with element mapping, were recorded using the accompanying AZTEC software.

### Raman confocal microspectroscopy

Raman confocal microspectroscopy was used to identify mineral species and the presence of organic matter in the samples as well as characterizing peak temperatures for the fossils. Raman spectra were collected at the Department of Materials and Environmental Chemistry (MMK)—Stockholm University (SU) using a Horiba LabRAM HR 800 Raman spectrometer equipped with an air-cooled double-frequency Nd:YAG laser operating at 532 nm. All *Prototaxites* samples were mounted on glass slides and exposed to a laser power of 5 mW through an objective lens with 50× magnification (NA 0.42). A diffraction grating with 600 grooves $mm^{-1}$ was used to resolve the spectra. Acquisition time was set between 2 and 4 s, with 30–50 scans accumulated from 100 to 3400 $cm^{-1}$ with a spectral resolution of 2 $cm^{-1}$ for obtaining the spectra. Five to ten spectra were taken from different parts of each sample.

Spectra postprocessing was performed with Origin 2021 (OriginLab Corp., Northampton, MA, USA), and a linear baseline was created for baseline correction, using fixed points at the shoulders of each visible band. Band deconvolution in the range 1000–1800 $cm^{-1}$ was performed using an iterative procedure with Multiple Peak Fit, using a Gaussian function, until fit converged with $R^2 \geq 0.997$.

**Fig. 1.** Saprophytic fungi from the Tyresta National Reserve, Stockholm, Sweden, sampled in September 2021 used to extract fungal isolates (A) T4 (*Armillaria mellea*), (B) T8 (*Postia rennyi*), and (C) T9 (*Fomitopsis pinicola*). (D) Isolate in Petri dish. Note the predominant growth as rhizomorph and (E) detailed image of one rhizomorph. (F) Microphotograph of a cut rhizomorph showing the hollow interior.

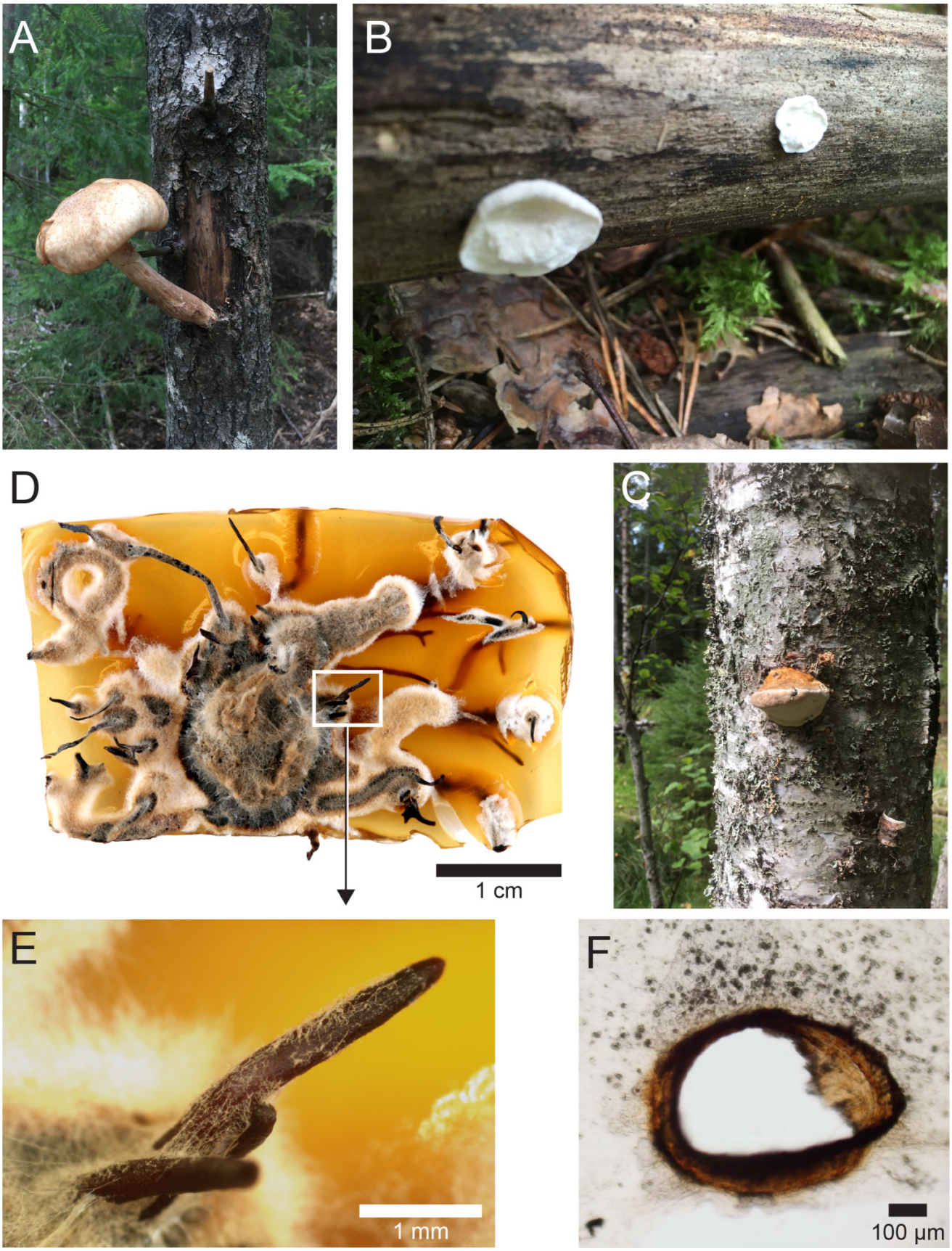


Can. J. Microbiol. Downloaded from cdnsciencepub.com by 90.190.215.226 on 05/14/24

Can. J. Microbiol. Downloaded from cdnsciencepub.com by 90.190.215.226 on 05/14/24

### FTIR microscopy

An FTIR microscope was used to characterize the mineralogical and organic content of the fossils, and used as basis for calculating the $R_{3/2}$ value that reflects the lipidic composition of cellular membranes among different organisms, thus enabling determination of biological affinity (Igisu et al. 2009). FTIR spectra were recorded at MMK—SU, on a Varian 670-IR microscope equipped with a motorized *x*–*y*–*z* stage and a mercury cadmium telluride detector cooled with liquid nitrogen. The spectra were collected in both transmission and attenuated total reflectance (ATR) modes with a diamond ATR element. The infrared transmission spectra of the thin section from the Bordeaux quarry *Prototaxites* and extant fungi isolates were recorded with a 100 μm × 100 μm aperture and using a $CaF_2$ window. The infrared spectra in ATR mode were taken directly from a selected darker area of the Heider quarry *Prototaxites* fossil sample. For each spectrum, 256 scans were accumulated at a spectral resolution of 4 $cm^{-1}$, and they were recorded in the frequency range of 600–4000 $cm^{-1}$. Finally, spectra from three to five locations in each sample were taken, and IR background spectra were taken before each sample. Spectra processing and further data analyses were performed with Origin 2021 (OriginLab Corp.). No baseline correction was necessary.

### 3D XRM

One cubic centimetre of the *Prototaxites* sample (Je-Sch0263) was cut for scanning using a 3D X-ray microscope (XRM). Scanning was carried out at the Stockholm University Brain Imaging Centre (SUBIC) using the ZEISS Xradia Versa 520 X-ray microscope. The sample was placed in a 14 mL Falcon round bottom polypropylene test tube packed with polystyrene packing material to keep the sample stable during scanning. The following scan parameters were used: 140 kV at 10 W with a 4 s exposure time. A total of 1601 projections were taken in full 360° rotation. A 4× objective was used to image a pixel size of 1.6 μm. Scanning was completed using Xradia Scout & Zoom software. The reconstructed .tiff stack was imported and visualized using Object Research Systems (ORS) (Montreal, Quebec, Canada) Dragonfly software using a non-commercial license.

## Results and interpretation

### Modern rhizomorph morphology

Here we present the results for the fossil *Prototaxites*, using modern fungus as an analogue. We compare and contrast results from other studies with our own observations of morphological and anatomical similarities between *Prototaxites* and modern rhizomorphs. At subsampling, the isolated fungus in T4 produced rhizomorphs ~1 mm wide and 3–5 cm long (Figs. 1D–1F). Rhizomorphs were visualized by ESEM (Figs. 2A–2C) and staining with CalcoFlourWhite using fluorescence microscopy (Figs. 2D and 2E). Each rhizomorph consists of a bundle of thousands of parallel-fused hyphae forming a tissue-like substrate at the margins surrounding a central cavity (Figs. 1D and 1E). The tubular elements are several centimetres long and 1–8 μm in diameter. The internal architecture of the studied modern rhizomorphs is characterized by a peripheral zone of parallel-bundled hyphae fused into a tissue-like substrate that surrounds a central cavity.

### *Prototaxites* morphology

The tubular elements (7–10 μm in diameter) of *Prototaxites* are clearly visible (Figs. 3A–3D) and occur in bundles divided by growth increments. The density, diameter, and wall thickness of the tubular structures and the width of the growth increments vary between specimens. The tubes are "spaghetti-like" in longitudinal section, unbranched, and aseptate (Fig. 3D).

The *Prototaxites* specimen from the Heider quarry has tubular structures that occur as alternating light and dark bands in cross section (Fig. 3A). The lighter bands consist of tubular structures with diameters up to ~50 μm, while the darker bands consist of tubular structures with diameters of ~10 μm (Figs. 3B–3D). According to the ESEM (Fig. 5) and Raman spectroscopy (Fig. 6), the lighter bands consist of quartz, while the darker bands consist of organic matter alternated with quartz.

The *Prototaxites* specimens from the Bordeaux quarry exhibit growth increments (Figs. 4A and 4B). Well-preserved tubular structures are found throughout (Figs. 4B–4D). In cross section, these are circular or near-circular with diameters up to ~10 μm (Figs. 4E and 4F), also consisting of quartz.

ESEM imaging reveals the lighter bands to be more homogeneous relative to the darker bands (Figs. 5A–5G). The dark bands are somewhat heterogeneous with abundant carbonaceous matter in between the quartz. Element mapping highlights abundant C in the bands between the quartz, and occasional traces of Ca (Figs. 5E and 5F).

In the centre of most tubes, a dark circular nuclei-like structure, 1–2 μm in diameter, is seen in cross section (Figs. 3E–3G). These structures are detected in most tubes when analysing the fossil in cross section and we interpret them as contracted, fossilized cell content (organelles).

### Raman spectroscopy

Overall, the Raman spectra of the *Prototaxites* fossils show the presence of bands in the first- and second-order regions of the Raman spectra (Figs. 6A and 6B), characteristic of carbonaceous material (Kouketsu et al. 2014; Qu et al. 2015, 2018; Henry et al. 2019; Bonneville et al. 2020). The first-order Raman spectral region contains two main bands (1100–1800 $cm^{-1}$), whereas the second-order region is characterized by several overlapping bands (2400–3500 $cm^{-1}$), previously interpreted as overtones and inelastic scattering of the bands present in the first-order region (Henry et al. 2019). Additionally, bands at 125, 202, and 461 $cm^{-1}$ (Fig. 6B) are characteristic of quartz minerals (Chukanov and Vigasina 2020).

As expected, the carbonaceous material occurs mainly in the darker regions of the Heider quarry fossil (Fig. 6D). In the first-order region of the spectra, the graphite (G) band is commonly attributed to in-plane vibrations of carbon atoms and is observed at ~1600 $cm^{-1}$ (Qu et al. 2018; Henry et al. 2019; Bonneville et al. 2020). The disordered (D) band occurs at ~1350 $cm^{-1}$, and corresponds to ring breathing mode in disordered carbonaceous material (Henry et al. 2019).

**Fig. 2.** Photomicrographs and ESEM images of modern rhizomorph from sample T4. (A) ESEM image of a rhizomorph showing the longitudinal growth direction of the hyphae. (B) Cross section through rhizomorph. The central cavity has collapsed due to vacuum in the ESEM chamber. (C) Close-up of the cross section. Note the varying diameter of the tubular structures. (D, E) Selected parts of rhizomorphs stained with ClacoFlourWhite and studied using fluorescence microscopy. (D) Tip of rhizomorph. (E) Note the longitudinal direction of the hyphae.

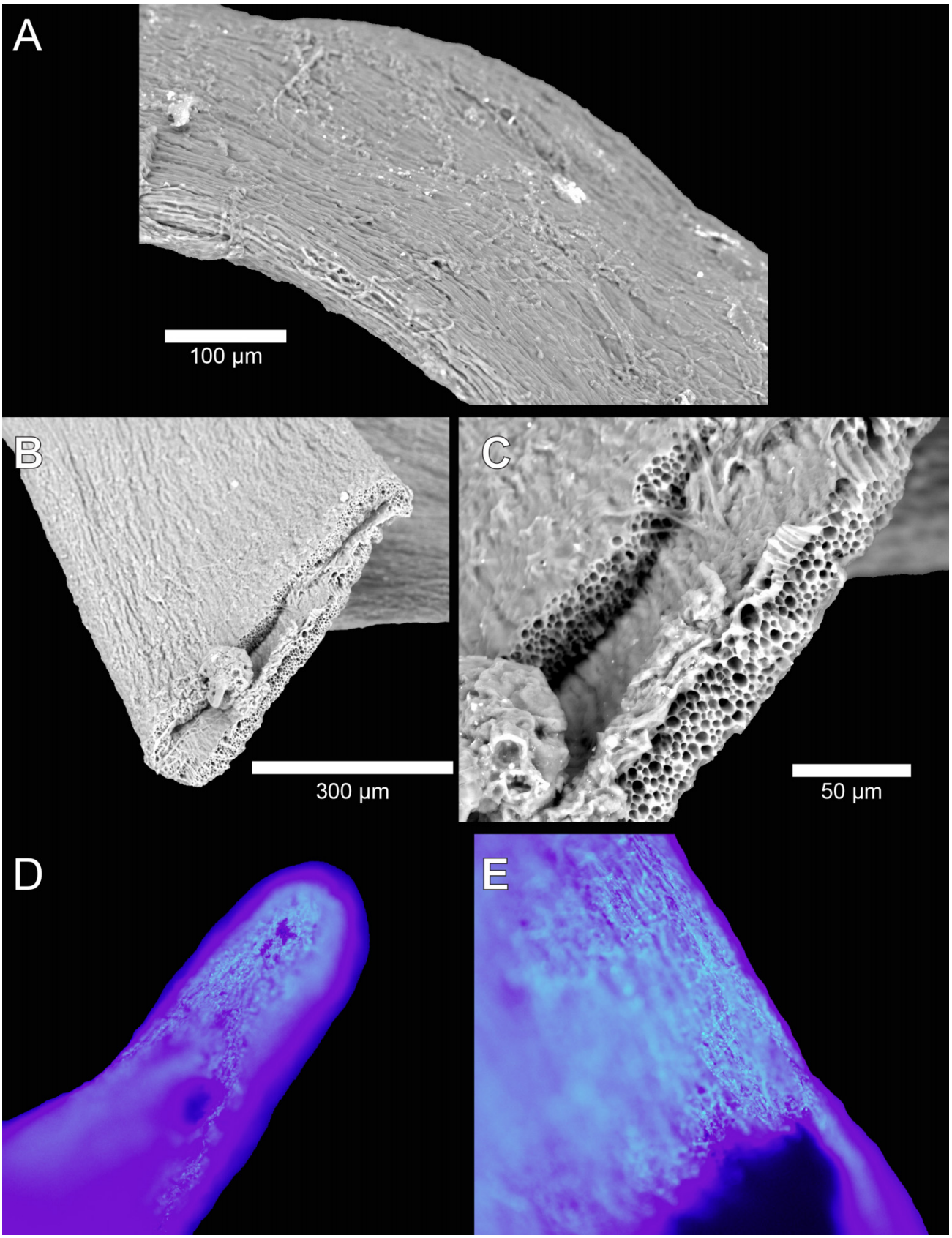


Can. J. Microbiol. Downloaded from cdnsciencepub.com by 90.190.215.226 on 05/14/24

**Fig. 3.** Micrographs of *Prototaxites*, sample JE-Sch0252 from Heider quarry. (A) Overview of a thin section of *Prototaxites* in transverse section; note the shift between the more organic-rich dark bands and quartz-dominated light bands. Cell size/crystallinity increases with age from left to right. Darker bands get darker with age as well. (B, C) Micrograph, close-up of tubes in transverse section. (D) Micrograph with close-up of the tubular structures, longitudinal section. Light band surrounded by two darker bands. Cell diameter is larger in the bright band compared with dark bands. The possible cell nuclei are more commonly visible in the darker bands. Red arrows point to nuclei in bright bands. (E) Micrograph of *Prototaxites* cross section, boundary between light and dark bands. Note the presence of dark specks, possible cell content. (F, G) Possible cell content (arrows) preserved in the quartz-rich bright bands. (H) A large *Prototaxites* specimen Je-Sch2318 from Heider quarry.

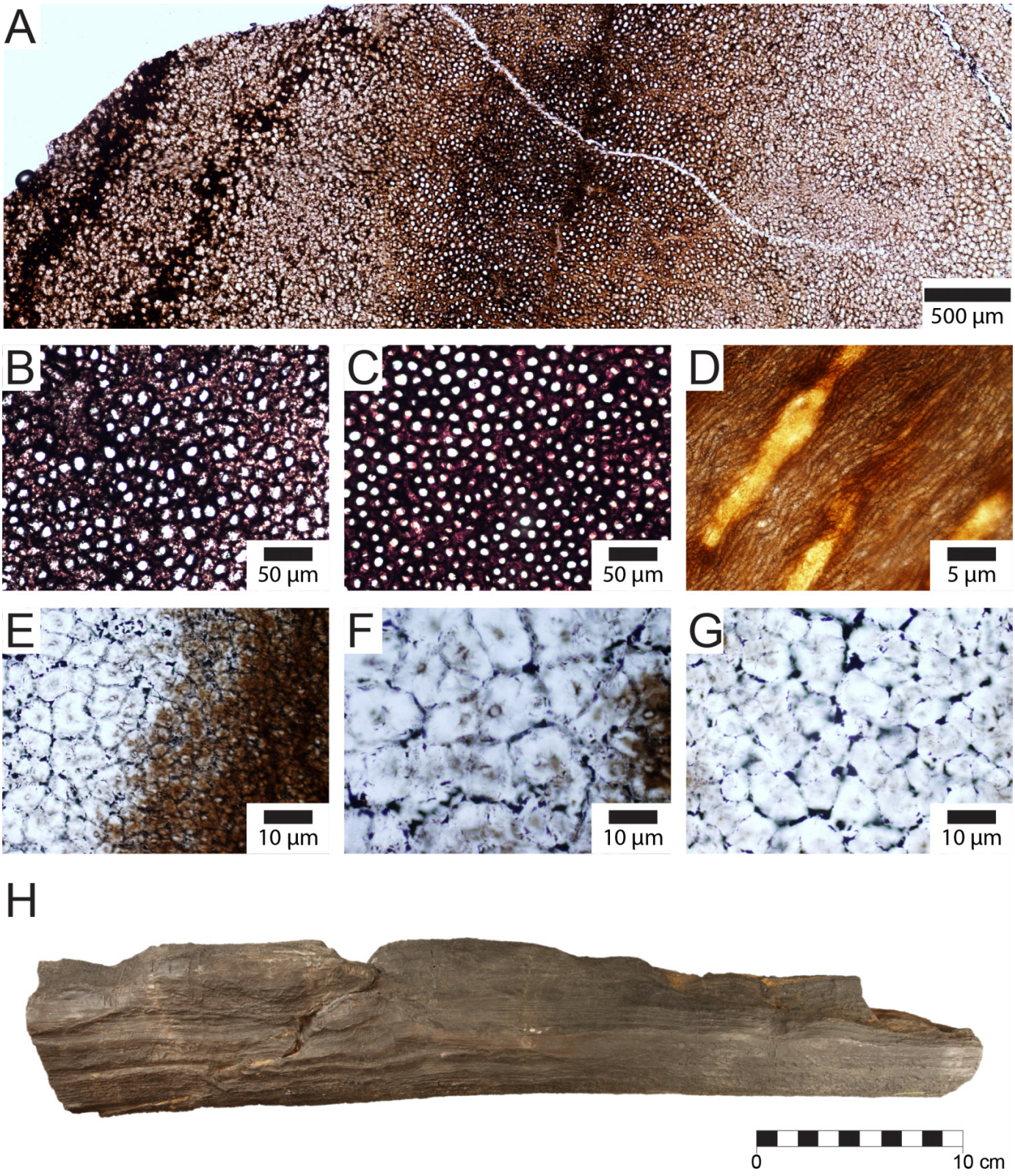


Can. J. Microbiol. Downloaded from cdnsciencepub.com by 90.190.215.226 on 05/14/24

**Fig. 4.** Bordeaux quarry specimens of *Prototaxites*. (A, B) *Prototaxites* specimen S004496 displaying growth increments. (C, D) Micrograph with close-up of the tubular structures, longitudinal section of specimen S04496-04 and S04496-05. (E, F) Micrograph, close-up of tubes in transverse section of specimen S082540.

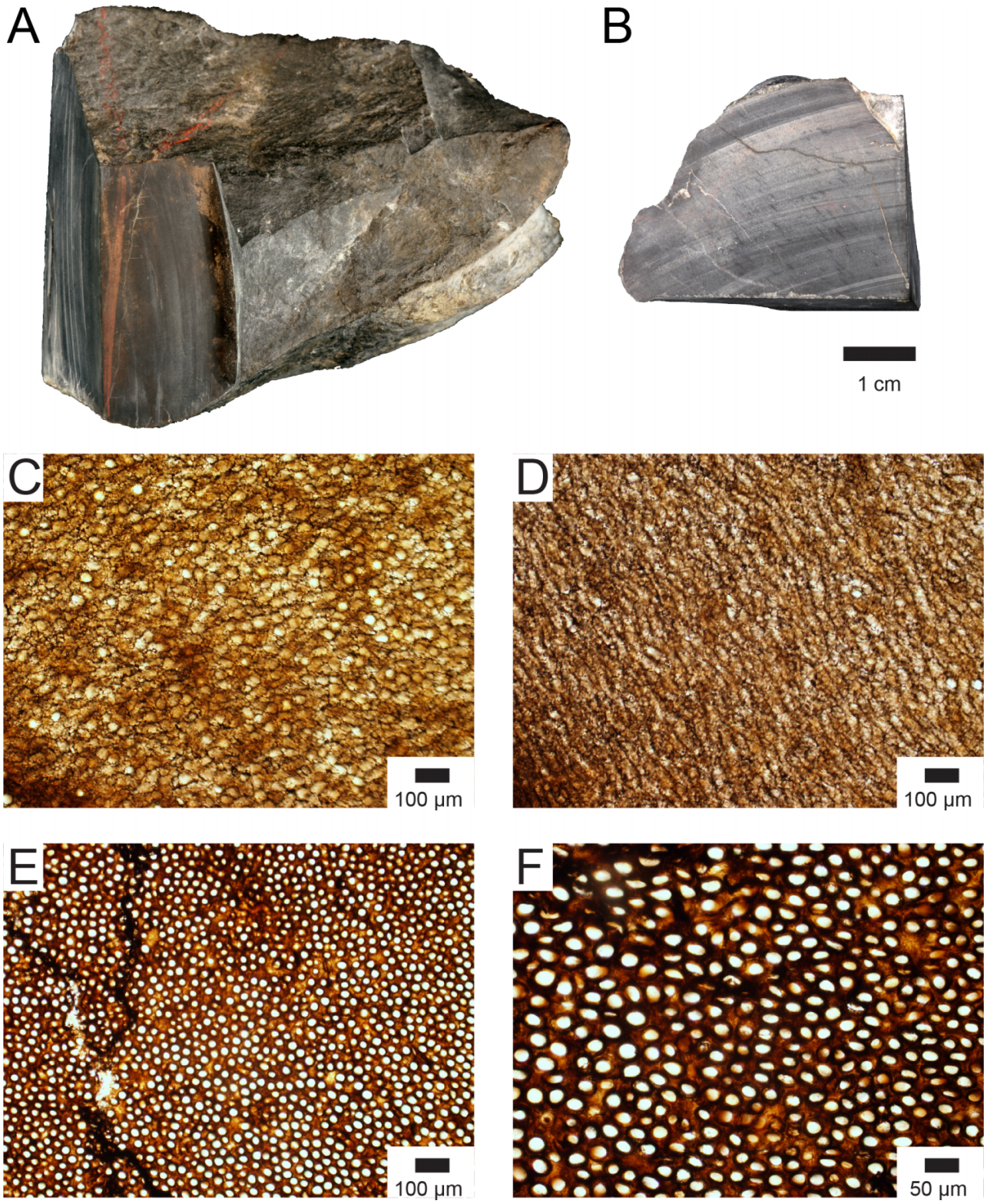


Can. J. Microbiol. Downloaded from cdnsciencepub.com by 90.190.215.226 on 05/14/24

**Fig. 5.** ESEM micrographs of *Prototaxites*, sample JE-Sch0252 from Heider quarry. (A) Overview showing the distribution of bands seen in ESEM. Bands that appear dark in optical microscopy appear more heterogeneous and with more inclusions of carbonaceous matter in between the quartz crystals when using ESEM (top and bottom sides of dashed lines). Light bands are more homogeneous (in between dashed lines). (B) Composite image of element mapping. (C) Si K series elemental mapping. (D) O K series elemental mapping. (E) Ca K series elemental mapping. (F) C K series elemental mapping. (G) S K series elemental mapping.

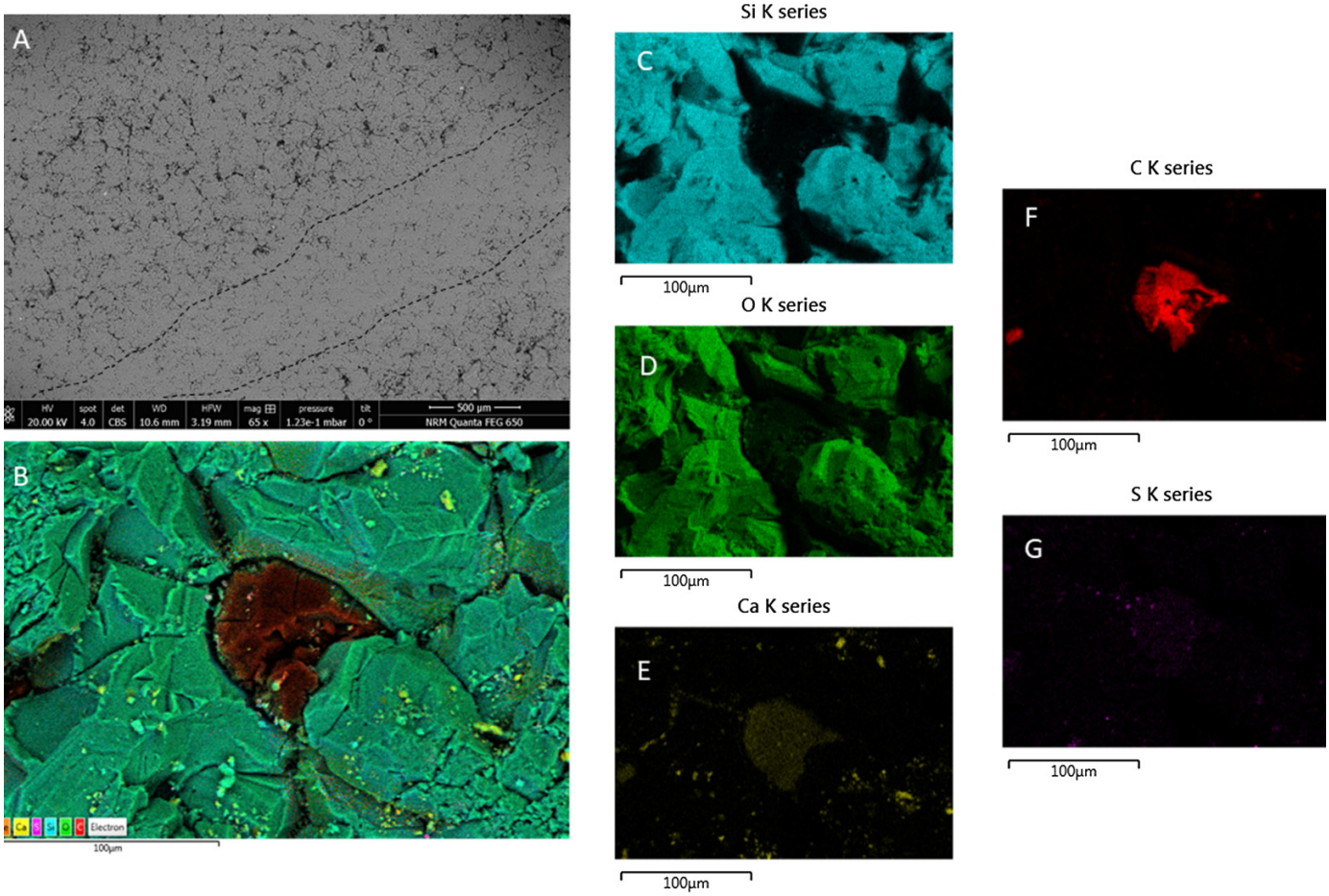


Deconvolution of the two bands in this region showed the presence of the D1 and G bands, together with the following additional bands: D2, D4, D5, and D6 (Fig. 7A; Henry et al. 2019), which indicates that the fossil reached low- to medium-grade thermal maturity (Kouketsu et al. 2014; Bonneville et al. 2020). Using the FWHM-D1 relationship determined by Kouketsu et al. (2014), the peak temperature experienced by the fossil was calculated to be 269 ± 14 °C.

The difference in the Raman intensity between the darker regions from which the spectra were acquired suggests that the amount of organic matter varies within these regions. The fringes are artefacts, most likely caused by internal reflections of the fossil and (or) glass slides. In contrast, the spectra of the brighter parts of the fossil (Fig. 6E) did not show bands corresponding to carbonaceous materials. Instead, these areas are characterized by a stronger band at ~460 $cm^{-1}$ and a medium band at ~200 $cm^{-1}$ bands, both corresponding to vibrational modes of quartz.

The Bordeaux quarry fossil is entirely composed of dark carbonaceous matter. The deconvolution of the Raman bands in the first-order region shows the presence of the two main bands D1 and G and three additional bands D3, D4, and D5 (Fig. 7B), indicating that this fossil consists mainly of low-grade carbonaceous material. Again, using the FWHM-D1, the peak-metamorphic temperature was calculated to be 128 ± 10 °C.

Finally, Raman 1350–1600 $cm^{-1}$ intensity ratios ($I$ (1350)/$I$ (1600)) were previously used to estimate the structural order of carbonaceous matter (Kouketsu et al. 2014; Qu et al. 2015). In our study, this ratio was calculated considering only the intensity of the two main bands, regardless of the resultant deconvolution bands. As a result, the fossils from the Heider and Bordeaux quarries have intensity ratios of 0.62 ± 0.03 and 0.72 ± 0.01, respectively, indicating the presence of organic matter with lower structural order.

## FTIR

Infrared spectra were acquired for *Prototaxites* from both localities (Fig. 8). For the Heider quarry *Prototaxites*, no bands corresponding to organic matter were observed. The bands at

Can. J. Microbiol. Downloaded from cdnsciencepub.com by 90.190.215.226 on 05/14/24

**Fig. 6.** Confocal Raman spectra acquired from *Prototaxites*, sample JE-Sch0252 from Heider quarry. (A) Representative Raman spectrum of the carbonaceous matter in the fossils, with characteristic bands in the first- and second-order regions. The spectrum also indicates the presence of quartz mineral. (B) Two main bands from carbonaceous matter in the first-order region, the disordered band (D) at 1357 $cm^{-1}$ and the graphite band (G) at 1605 $cm^{-1}$. Characteristic quartz bands also appear at 461, 202, and 125 $cm^{-1}$. (C) Thin section of Heider quarry *Prototaxites*. The darker areas 1–5 correspond to the areas from which Raman spectra were collected for analysis. The Raman spectra from brighter areas i–iv were also acquired for comparison. (D) Raman spectra 1800–300 $cm^{-1}$ of the areas 1–5, indicating the presence of carbonaceous matter and quartz. This contrasts with the spectra of areas i–iv (E), which did not show bands of carbonaceous matter, presenting only bands at ~460 and ~200 $cm^{-1}$ characteristic of vibrational modes of quartz.

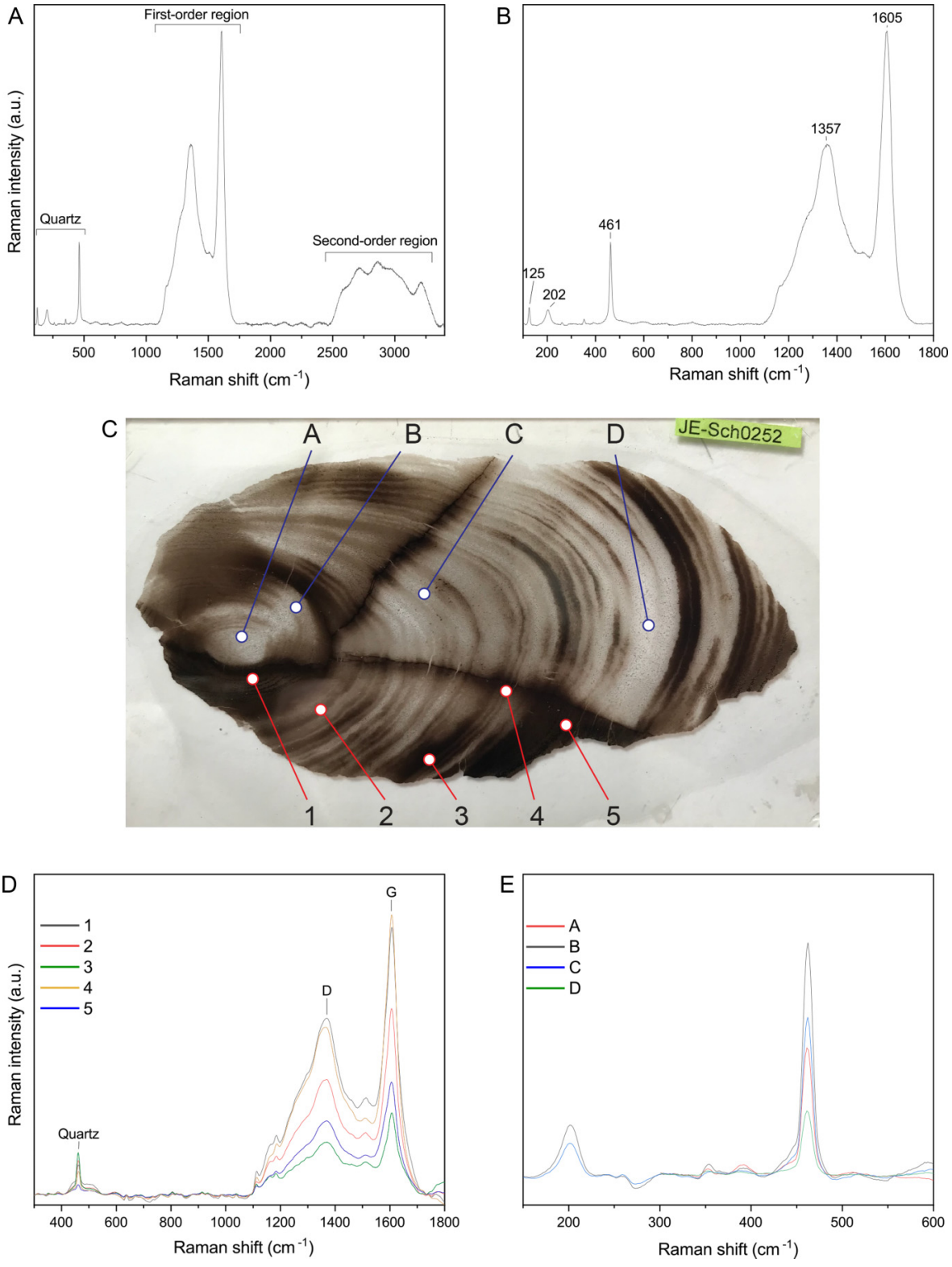


Can. J. Microbiol. Downloaded from cdnsciencepub.com by 90.190.215.226 on 05/14/24

**Fig. 7.** Representative Raman spectra illustrating the deconvolution of the D and G bands for the *Prototaxites* fossils from both Heider and Bordeaux quarries. (A) Deconvolution into D1, D2, D4, D5, D6, and G for the Raman spectra acquired of the Heider quarry fossils. (B) Deconvolution into D1, D4, D5, D6, and G for the Raman spectra acquired of the Bordeaux quarry fossils. In both cases, the FWHM-D1 was used for calculating the peak temperature experienced by the fossils, using the relationship determined by Kouketsu et al. (2014).

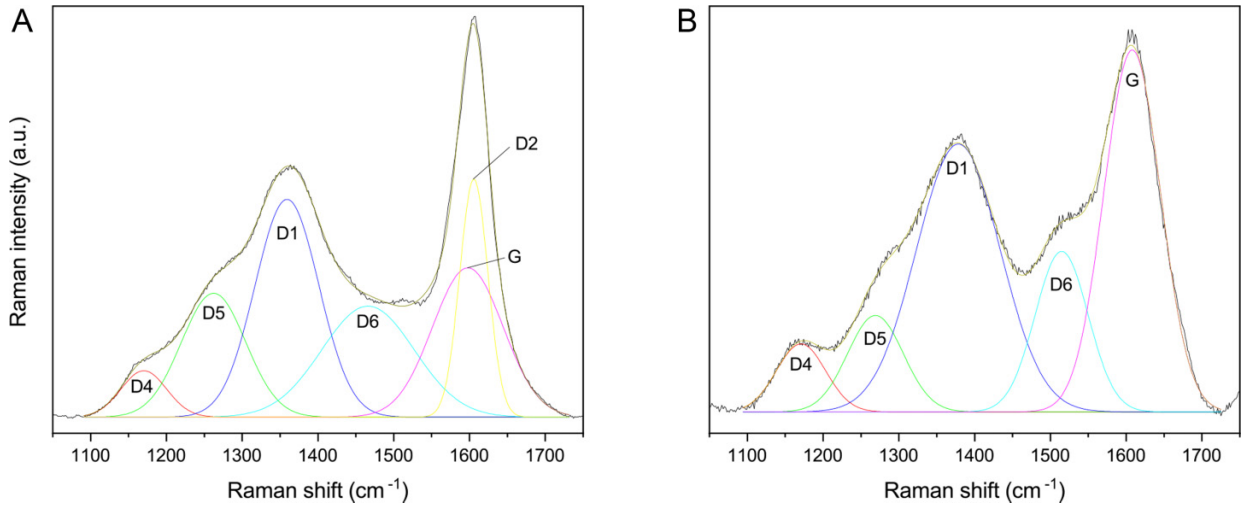


1087, 798, 695, and 460 $cm^{-1}$ indicate the presence of mainly organosilicon compounds, more specifically siloxanes, with Si–O–Si, Si–O–C, and Si–$CH_3$ groups (Socrates 2001; Benning et al. 2004; Launer and Arkles 2013).

For the Bordeaux *Prototaxites* sample, the 2950, 2925, and 2870 $cm^{-1}$ bands correspond to the asymmetric stretch of methyl ($v_{as}$ $CH_3$) and asymmetric and symmetric stretches of methylene ($v_{as}$ $CH_2$ and $v_s$ $CH_{2)}$. The bands at wavenumbers lower than 2500 $cm^{-1}$ (1990, 1870, 1790, 1680, 1620, 1520, and 1490 $cm^{-1}$) correspond to Si–O vibrations of quartz (Igisu et al. 2009; Qu et al. 2015), which masked the other signals from the organic matter—hampering a direct comparison of composition between the spectra of *Prototaxites* fossils and extant fungi (Fig. S1). As an alternative, the bands in the 3000–2800 $cm^{-1}$ can be used as follows: FTIR bands corresponding to $CH_3$ and $CH_2$ asymmetric stretches in the spectral region 2800–3000 $cm^{-1}$ were previously used to calculate the branching index of aliphatic chains $R_{3/2}$ (Igisu et al. 2009). For the extant fungi isolates T4, T8, and T9, the $R_{3/2}$ values obtained were 0.90 ± 0.05 ($n$ = 4), 0.950 ± 0.002 ($n$ = 4), and 0.90 ± 0.02 ($n$ = 5), respectively. The value obtained for the more well-preserved fossil *Prototaxites* from the Bordeaux quarry was 0.97 ± 0.01 ($n$ = 9), fitting the values for the extant fungi analysed. The high values (>0.5) observed for both the fossil and extant organisms indicate the prevalence of methyl groups over methylene-chain structure, i.e., highly branched aliphatic compounds.

## Discussion

The enigmatic fossil *Prototaxites loganii* Dawson encountered from Silurian to Upper Devonian successions was in the early days of its discovery interpreted as a conifer trunk, and although that hypothesis has been disregarded (Retallack and Landing 2014; Honegger et al. 2018, and references therein), there is still an ongoing debate concerning their affinity with groups such as red and brown algae, liverworts, fungi, and lichens put forward as the most possible parent organisms.

Our geochemical and morphological analyses of the enigmatic fossil *Prototaxites loganii* Dawson provide some new results.

The morphological and anatomical similarities between the studied *Prototaxites* and modern rhizomorphs are striking; both consist of tubular structures of similar length and diameter, fused together into a tissue-like material. Rhizomorphs are among the most complex organs produced by fungi, and are the result of a coordinated growth of millions of bundled hyphae. They are root-like structures constituted by a series of differentiated tissues, each with a distinctive hyphal type, orientation, size, and function. The dense tissue-like peripheral zones of the rhizomorphs correspond to the dark bands of the Heider quarry *Prototaxites* and are characterized by abundant carbonaceous material and poorly crystalline quartz, whereas the hollow interior of the rhizomorphs corresponds to the lighter bands of *Prototaxites* mineralized by quartz and lacking carbonaceous material. The lighter parts of *Prototaxites* likely represent earlier hollow vessels of the massive structures that were mineralized by quartz upon fossilization. The circular centralized structure within some crystalline cell walls from the Heider quarry sample may represent cell wall decay products enclosed by quartz precipitated from fluids supersaturated with silica during rapid permineralization, which is common in permineralized cell lumens. Fossilized fungi commonly display a central strand throughout hyphae, which could be diagenetic owing to shrinkage of the cell cytoplasm during the fossilization process (Ivarsson et al. 2012). We contend that *Prototaxites* thus represents giant fossil versions of modern rhizomorphs and

Can. J. Microbiol. Downloaded from cdnsciencepub.com by 90.190.215.226 on 05/14/24

**Fig. 8.** Representative FTIR spectra acquired for *Prototaxites* fossils from both Bordeaux and Heider quarries. Upper figure: The IR spectrum was acquired in the transmission mode from a thin section of the Bordeaux quarry fossil, and it is characterized by aliphatic bands between 3000 and 2800 $cm^{-1}$ and bands corresponding to Si–O vibrational modes of quartz. The box between 3050 and 2750 $cm^{-1}$ was enlarged to highlight the aliphatic bands at 2950 and 2925 $cm^{-1}$, which correspond to asymmetric stretching modes of methyl and methylene, respectively. Their intensity was used to calculate the $R_{3/2}$ ratio to determine the carbon chain branching. Lower figure: The IR spectrum on the bottom was acquired from the Heider quarry fossil using an ATR mode. Bands characteristic of organosilicon compounds were obtained, possibly indicating elemental substitution by incorporation of silicon atoms from the environment during the fossilization process.

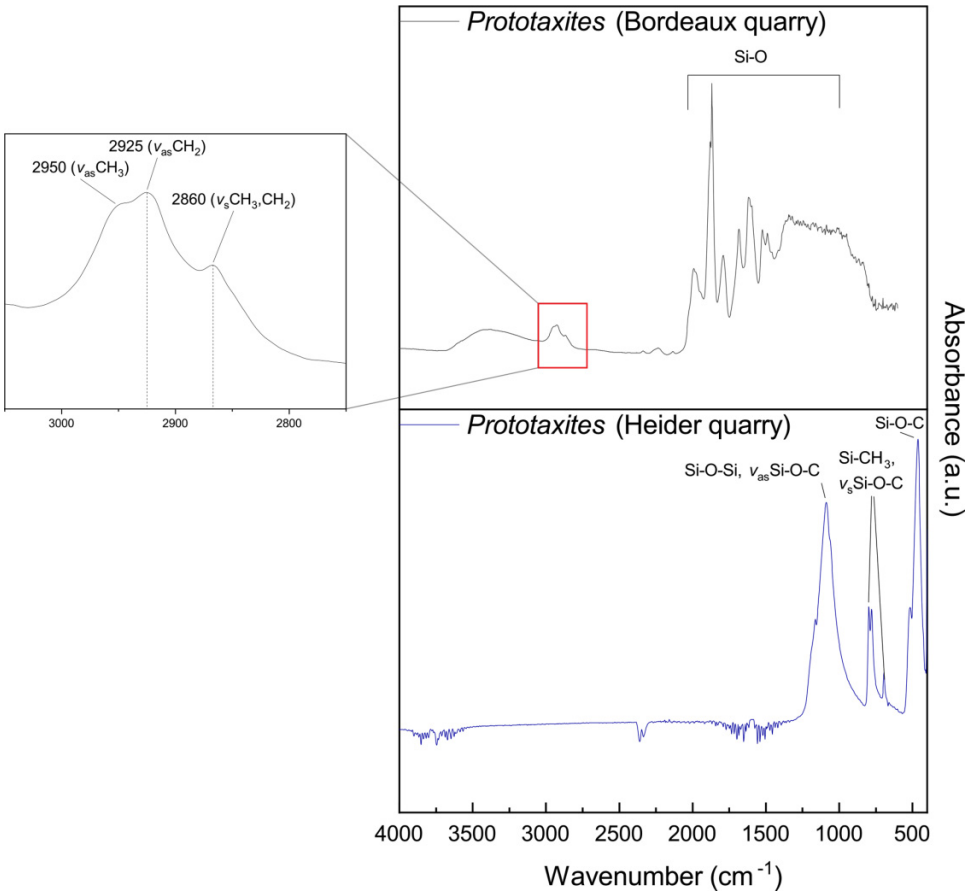


that the internal structure and morphology indicate that the fossils represent a complex growth structure based on fused hyphae. The Raman results for the *Prototaxites* sample from the Bordeaux quarry reveal—based on the fact that the G and D2 bands are merged into a single band—that this fossil is composed mainly of low-grade organic matter. In contrast, the Heider quarry fossil presents a clear separation between the G and D2 bands. The presence of both bands has previously been recognized as an indication that the fossil experienced temperatures high enough to partially transform the organic matter into anthracite (Straka and Sýkorová 2018), which agrees with the different thermal maturation temperatures calculated for each fossil of 128 ± 10 and 269 ± 14 °C, respectively. This could also explain the results obtained by FTIR for the Heider quarry fossil, which did not show any remains of aliphatic vibrations containing, e.g., carbonyl or alkene groups. The spectra showed the presence of organosilicon compounds, suggesting that this fossil might have undergone elemental substitution, incorporating silicon atoms from the hydrothermal environment around it during its permineralization process. This is further supported by the lack of contrast in the XRM data. Although the data do show some small inclusions within the host rock, the imaging of *Prototaxites* itself was unsuccessful. This is likely due to the lack of contrast between the mycelia structures, surrounding fossilized organic material, and the host rock.

The *Prototaxites* sample from Bordeaux quarry, on the other hand, showed remains of aliphatic compounds, facilitating the calculation of its $R_{3/2}$ ratio (0.97 ± 0.01). The $R_{3/2}$ values reflect the lipidic composition of the membrane cells of the different organisms, possible to tell apart due to the distinct lipids' structure (Igisu et al. 2009). Previous studies on thermal alteration of aliphatic C–H bonds during simulated diagenesis on extant organisms showed that the change in both aliphatic $CH_2$ and $CH_3$ bonds is delayed in the presence of silica (Igisu et al. 2018). Igisu et al. (2018) also showed that the $R_{3/2}$ values of the altered organism did not

Can. J. Microbiol. Downloaded from cdnsciencepub.com by 90.190.215.226 on 05/14/24

**Fig. 9.** Comparison between the $R_{3/2}$ and $I$ (1350)/$I$ (1600) values for the *Prototaxites* fossils, eukaryotic and prokaryotic organisms. (A) $R_{3/2}$ ratio comparison of obtained values for extant fungi and the *Prototaxites* fossils (this study), and previously published values for extant plants, algae, bacteria, and cyanobacteria (Igisu et al. 2009). (B) $I$ (1350)/$I$ (1600) versus $R_{3/2}$ values of *Prototaxites* fossil (purple; this study) and previously published values for fossil eukaryotes (green area; Qu et al. 2015) and fossil prokaryotes (red area; Igisu et al. 2009; Qu et al. 2015).

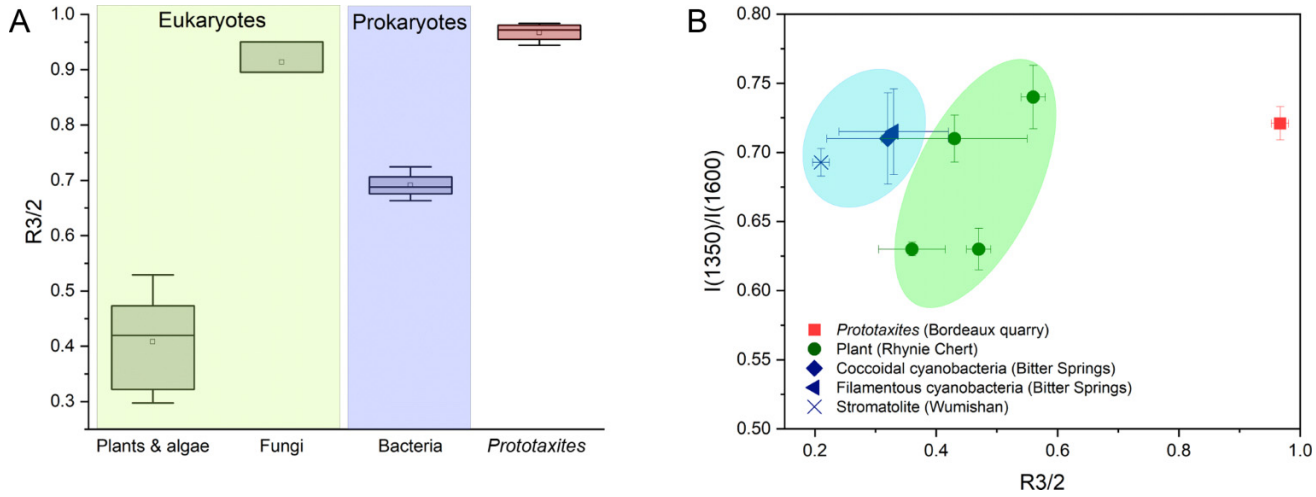


**Fig. 10.** Illustration of the authors' palaeoenvironmental and morphological interpretation of *Prototaxites* thriving in a Devonian landscape. It is likely that *Prototaxites* explored land by foraging through sediment, soil, and aquatic environments.

significantly change when compared to the living organism, having at most slightly increased. Analogously, despite undergoing diagenesis, the calculated $R_{3/2}$ value of fossil *Prototaxites* (0.97 ± 0.01) is likely to have remained close to the living organism, due to a delay caused by the presence of silica. When considering the ratio calculated for the extant fungi analysed in this study (average 0.915 ± 0.008) and the values found in the literature for extant plants and

Can. J. Microbiol. Downloaded from cdnsciencepub.com by 90.190.215.226 on 05/14/24

Can. J. Microbiol. Downloaded from cdnsciencepub.com by 90.190.215.226 on 05/14/24

bacteria/cyanobacteria (0.41 ± 0.09 and 0.69 ± 0.03, respectively; Igisu et al. 2009; Bonneville et al. 2020), the similarity between *Prototaxites* and fungi is further supported (Fig. 9A).

Moreover, a combination between the *I* (1350)/*I* (1600) and the branching index of aliphatic chains $R_{3/2}$ was recently used to differentiate prokaryotes and eukaryotes, as their cellular content and structure vary sufficiently, resulting in a different trend between the two groups (Igisu et al. 2009; Qu et al. 2015, 2018; Bonneville et al. 2020). When considering both $R_{3/2}$ and *I* (1350)/*I* (1600) mentioned for the Bordeaux quarry *Prototaxites*, and comparing our results with the *I* (1350)/*I* (1600) versus $R_{3/2}$ signatures of previously reported eukaryotic (plants from Rhynie chert) and prokaryotic organisms (cyanobacteria from Bitter Springs and a stromatolite from Wumishan) (Igisu et al. 2009; Qu et al. 2015, 2018), the *Prototaxites* fossil falls clearly outside the range of prokaryotes, being closer to the eukaryotic range (Fig. 9B). *Prototaxites*, however, falls also outside the field indicated for eukaryotes in Fig. 9B, since the latter is based only on data presently available for plants. A broader study of eukaryotic organisms, especially fungal *I* (1350)/*I* (1600) versus $R_{3/2}$ signatures, could in the future provide more detailed knowledge on *Prototaxites* affinity within fungi.

Based on the morphology of *Prototaxites* and the FTIR data collected, and combined with results from previous studies (Boyce et al. 2007), we conclude that the *Prototaxites* specimens of both Heider quarry and Bordeaux quarry most likely are fungi. These fungi represent extinct giant forms of vegetative growth structures, similar to modern complex mycelial growth forms, such as cords and rhizomorphs. Owing to their similarity to tree trunks, it has been assumed that *Prototaxites* grew vertically. However, there are no conclusive results that support this assumption. Furthermore, we were unable to locate any mention of in situ vertical stumps in the previous literature, and the variations in diameter from stump to tip seen in most illustrations cannot be corroborated by publications except one, where the measured difference in diameter from base to tip is just a few decimetres (Hueber 2001). Considering our new data, it is possible that *Prototaxites* had a more varied spatial growth habit and that it was just as likely to grow horizontally as it was to grow vertically. The functions of both mycelia and rhizomorphs are both explorational and for translocation of nutrients, water, and oxygen from nutrient-rich to nutrient-poor environments (Yafetto 2018), thus enhancing the survival of fungi in nutrient-limited settings. It is likely that *Prototaxites* explored land by foraging through sediment, soil, and aquatic environments. It likely grew underground and, on the surface, perhaps even in the air, but strictly vertical growth on an otherwise barren or little-vegetated landscape seems unlikely (Fig. 10).

The proximity to areas with volcanic activity and hot springs might explain the preservation by silica, which is also supported by the occurrence of coarse-grained volcaniclastic rocks dated to the early Pragian to early Emsian (Kennedy et al. 2013). Hydrothermal silica-oversaturated fluids probably impregnated the *Prototaxites* rhizomorphs leading to exceedingly rapid permineralization. This may be the reason for the high grade of preservation and the maintenance of the original anatomy down to cellular level. Similar examples of rapid permineralization preserving exceptionally delicate features, such as nuclei and starch grains of osmundaceous ferns and fungal hyphae, are known from hydrothermally influenced deposits of southern Sweden (Bomfleur et al. 2014; McLoughlin and Bomfleur 2016). It is likely that geothermal springs and associated groundwaters oversaturated by silica could have been of importance for the survival of these giant fungal growth structures. If local hot springs acted as havens of nutrients and accessible bioavailable carbohydrates in the form of dead or living plants in an otherwise plant-scarce environment, the growth of large rhizomorphic structures could translocate necessary nutrients from one area to another. Fungi may have mined nutrient-rich areas for minerals and organic matter to enable growth further away.

The ability to grow large translocation structures was probably an advantage for surviving in the sparsely vegetated Early Devonian ecosystems where nutritional sources were more scattered than in modern landscapes.

During the Early Devonian, terrestrial vegetation remained sparse and was represented essentially by herbaceous plants lacking secondary wood (Gerrienne et al. 2011) but evidence of fungal–plant interactions extend back to the Early Devonian, Rhynie chert (Strullu-Derrien et al. 2015, 2018).

At that time, the population of living plants and accumulations of dead plant matter available for fungal decomposition was meagre comparable to our modern world.

However, local areas of flourishing vegetation were probably sufficient to support the massive growth structures of *Prototaxites*, and perhaps their size enabled necessary water and nutritional translocations from nutrient-rich to nutrient-poor areas. In modern rhizomorphs, the function of the central cavity is mostly for translocating oxygen. To grow such a massive fungal structure as *Prototaxites*, high amounts of oxygen would have been required, suggesting that the core region of *Prototaxites* supplied the tissues with oxygen in the dysaerobic subsurface to form an early terrestrial aeration system. Thus, *Prototaxites* may have played a pivotal role in Early Devonian ecosystems by connecting nodes of vegetation, aerating subsurface tissues, and translocating key nutrients, through soils of an otherwise sparsely vegetated planet.

## Article information


### History dates

Received: 16 November 2021
Revised: 22 September 2022
Accepted: 20 October 2022
Accepted manuscript online: 13 December 2022
Version of record online: 13 December 2022



### Copyright

© 2022 The Author(s). This work is licensed under a Creative Commons Attribution 4.0 International License (CC BY 4.0), which permits unrestricted use, distribution, and reproduction in any medium, provided the original author(s) and source are credited.

Can. J. Microbiol. Downloaded from cdnsciencepub.com by 90.190.215.226 on 05/14/24

## Data availability

The specimens are part of the paleobotanical collections hosted at the Swedish Museum of Natural History (NRM). Data generated or analysed during this study are available from the corresponding author upon reasonable request.

# Author information


## Author ORCIDs

Vivi Vajda https://orcid.org/0000-0003-2987-5559
Ashley Krüger https://orcid.org/0000-0003-1196-8693


## Author notes

This paper is part of a collection entitled Astrobiology.

## Author contributions

Vivi Vajda: conceptualization, data curation, formal analysis, funding acquisition, investigation, methodology, project administration, writing – original draft, writing – review & editing; Larissa Lopes Cavalcante: data curation, formal analysis, investigation, methodology, validation, writing – original draft, writing – review & editing; Kristoffer Palmgren: formal analysis, investigation, methodology, writing – review & editing; Ashley Krüger: data curation methodology, visualization, writing – original draft, writing – review & editing; Magnus Ivarsson: conceptualization, formal analysis, investigation, methodology, project administration, supervision, writing – original draft, writing – review & editing.

## Competing interests

The authors declare there are no competing interests.


## Funding information

This research was supported by the Swedish Research Council grant VR 2019-4061 (V.V.) and the Knut and Alice Wallenberg Foundation grant KAW 2020.0145 (V.V.). XRM scanning data acquisition was supported by a grant to the Stockholm University Brain Imaging Centre (SU FV-5.1.2-1035-15).


# Supplementary material

Supplementary data are available with the article at https://doi.org/10.1139/cjm-2021-0358.

# References


Badawy, A.S., Mehlqvist, K., Vajda, V., Ahlberg, P., and Calner, M. 2014. Late Ordovician (Katian) spores in Sweden: oldest land plant remains from Baltica. GFF, **136**(1): 16–21. doi:10.1080/11035897.2014.899266.

Benning, L. G., Phoenix, V. R., Yee, N., and Konhauser, K. O. 2004. The dynamics of cyanobacterial silicification: an infrared micro-spectroscopy investigation. Geochim. Cosmochim. Acta, **68**(4): 743–757. doi:10.1016/S0016-7037 (03) 00488-5.

Bomfleur, B., McLoughlin, S., and Vajda, V. 2014. Fossilized nuclei and chromosomes reveal 180 million years of genomic stasis in royal ferns. Science, **343**(6177): 1376–1377. doi:10.1126/science.1249884. PMID: 24653037.

Bonneville, S., Delpomdor, F., Préat, A., Chevalier, C., Araki, T. Kazemian, M., et al. 2020. Molecular identification of fungi microfossils in a neoproterozoic shale rock. Sci. Adv. **6**(4): eaax7599. doi:10.1126/sciadv.aax7599. PMID: 32010783.

Boyce, C.K., Hotton, C.L., Fogel, M.L., Cody, G.D., Hazen, R.M., Knoll, A.H., and Hueber, F.M. 2007. Devonian landscape heterogeneity recorded by a giant fungus. Geology, **35**(5): 399–402. doi:10.1130/G23384A.1.

Chukanov, N.V., and Vigasina, M.F. 2020. Vibrational (infrared and Raman) spectra of minerals and related compounds. Springer International Publishing, Cham, Switzerland. p. 1141.

Dawson, J.W. 1859. On fossil plants from the Devonian rocks of Canada. Q. J. Geol. Soc. **15**(1–2): 477–488. doi:10.1144/GSL.JGS.1859.015.01-02.57.

Edwards, D, Morris, J.L, Richardson, J.B, and Kenrick, P. 2014. Cryptospores and cryptophytes reveal hidden diversity in early land floras. New Phytol. **202**: 50–78. doi:10.1111/nph.12645. PMID: 24410730.

Edwards, D., and Axe, L. 2012. Evidence for a fungal affinity for Nematasketum, a close ally of Prototaxites. Botanical Journal of the Linnean Society, **168**(1): 1–18, doi:10.1111/j.1095-8339.2011.01195.x.

Gerrienne, P., Gensel, P.G., Strullu-Derrien, C., Lardeux, H., Steemans, P., and Prestianni, C. 2011. A Simple Type of Wood in Two Early Devonian Plants. American Association for the Advancement of Science, **333**: 837. doi:10.1126/science.1208882.

Graham, L.E., Cook, M.E., Hanson, D.T., Pigg, K.B., and Graham, J.M. 2010. Structural, physiological, and stable carbon isotopic evidence that the enigmatic paleozoic fossil *Prototaxites* formed from rolled liverwort mats. Am. J. Bot. **97**(2): 268–275. doi:10.3732/ajb.0900322. PMID: 21622387.

Gray, J., Laufeld, S., and Boucot, A.J. 1974. Silurian trilete spores and spore tetrads from Gotland: their implications for land plant evolution. Science, **185**(4147): 260–263. doi:10.1126/science.185.4147.260. PMID: 17812053.

Gross, W. 1933. Die unterdevonischen fische und gigantostraken von overath. Abh. Preuß. Geol. Landesanst, **145**: 41–77.

Hagström, J., and Mehlqvist, K. 2012. The dawn of terrestrial ecosystems on Baltica: first report on land plant remains and arthropod coprolites from the Upper Silurian of Gotland, Sweden. Palaeogeogr. Palaeoclimatol. Palaeoecol. **317–318**: 162–170. doi:10.1016/j.palaeo.2012.01.001.

Henry, D.G., Jarvis, I., Gillmore, G., and Stephenson, M. 2019. Raman spectroscopy as a tool to determine the thermal maturity of organic matter: application to sedimentary, metamorphic and structural geology. Earth Sci. Rev. **198**: 102936. doi:10.1016/j.earscirev.2019.102936.

Honegger, R., Edwards, D., Axe, L., and Strullu-Derrien, C. 2018. Fertile *Prototaxites taiti*: a basal ascomycete with inoperculate, polysporous asci lacking croziers. Philos. Trans. R. Soc. B Biol. Sci. **373**(1739): 20170146–20170146. doi:10.1098/rstb.2017.0146.

Hueber, F.M. 2001. Rotted wood–alga–fungus: the history and life of *Protot axites* Dawson 1859. Rev. Palaeobot. Palynol. **116**(1): 123–158. doi:10.1016/S0034-6667 (01) 00058-6.

Igisu, M, Yokoyama, T, Ueno, Y, Nakashima, S., Shimojima, M., Ohta, H., and Maruyama, S. 2018. Changes of aliphatic C–H bonds in cyanobacteria during experimental thermal maturation in the presence or absence of silica as evaluated by FTIR microspectroscopy. Geobiology, **16**: 412–428. doi:10.1111/gbi.12294. PMID: 29869829.

Igisu, M., Ueno, Y., Shimojima, M., Nakashima, S., Awramik, S.M., Ohta, H., and Maruyama, S. 2009. Micro-FTIR spectroscopic signatures of bacterial lipids in proterozoic microfossils. Precambrian Res. **173**(1): 19–26. doi:10.1016/j.precamres.2009.03.006.

Ivarsson, M., Bengtson, S., Belivanova, V., Stampanoni, M., Marone, F., and Tehler, A. 2012. Fossilized fungi in subseafloor eocene basalts. Geology, **40**(2): 163–166. doi:10.1130/G32590.1.

Kennedy, K.L., Gibling, M.R., Eble, C. F., Gastaldo, R. A., Gensel, P.G., Wener- Zwanziger, U., and Wilson, R.A. 2013. Lower Devonian coaly shales of northern New Brunswick, Canada: plant accumulations in the early stages of terrestrial colonization. J. Sediment. Res. **83**: 1202–1121. doi:10.2110/jsr.2013.86.

Kouketsu, Y., Mizukami, T., Mori, H., Endo, S., Aoya, M. Hara, H., et al. 2014. A new approach to develop the Raman carbonaceous material geothermometer for low-grade metamorphism using peak width. Island Arc, **23**(1): 33–50. doi:10.1111/iar.12057.

Launer, P.J., and Arkles, B. 2013. Silicon compounds: silanes & silicones. Gelest, Inc., Morrisville, PA, USA. pp. 175–178.

Leslie, A.B., Simpson, C., and Mander, L. 2021. Reproductive innovations and pulsed rise in plant complexity. Science, **373**(6561): 1368–1372. doi:10.1126/science.abi6984. PMID: 34529461.

McLoughlin, S., and Bomfleur, B. 2016. Biotic interactions in an exceptionally well preserved osmundaceous fern rhizome from the Early Jurassic of Sweden. Palaeogeogr. Palaeoclimatol. Palaeoecol. **464**: 86–96. doi:10.1016/j.palaeo.2016.01.044.

Mehlqvist, K., Larsson, K., and Vajda, V. 2014. Linking Upper Silurian terrestrial and marine successions—palynological study from Skåne, Sweden. Rev. Palaeobot. Palynol. **202**: 1–14. doi:10.1016/j.revpalbo.2013.12.001.

Mehlqvist, K., Steemans, P., and Vajda, V. 2015. First evidence of Devonian strata in Sweden—a palynological investigation of Övedskloster drillcores 1 and 2, Skåne, Sweden. Rev. Palaeobot. Palynol. **221**: 144–159. doi:10.1016/j.revpalbo.2015.06.007.

Mehlqvist, K., Vajda, V., and Steemans, P. 2012. Early land plant spore assemblages from the Late Silurian of Skåne, Sweden. GFF, **134**(2): 133–144. doi:10.1080/11035897.2012.683451.

Nelsen, M.P., and Boyce, K. 2022. What to do with prototaxites? Int. J. Plant Sci. **183**(6). doi:10.1086/720688.

Qu, Y., Engdahl, A., Zhu, S., Vajda, V., and McLoughlin, N. 2015. Ultrastructural heterogeneity of carbonaceous material in ancient cherts: investigating biosignature origin and preservation. Astrobiology, **15**(10): 825–842. doi:10.1089/ast.2015.1298. PMID: 26496525.

Qu, Y., Zhu, S., Whitehouse, M., Engdahl, A., and McLoughlin, N. 2018. Carbonaceous biosignatures of the earliest putative macroscopic multicellular eukaryotes from 1630 Ma Tuanshanzi Formation, north China. Precambrian Res. **304**: 99–109. doi:10.1016/j.precamres.2017.11.004.

Retallack, G.J. 2001. *Scoyenia* burrows from Ordovician palaeosols of the Juniata Formation in Pennsylvania. Palaeontology, **44**(2): 209–235. doi:10.1111/1475-4983.00177.

Retallack, G.J. 2022. Ordovician–Devonian lichen canopies before evolution of woody trees. Gondwana Res. **106**: 211–223. doi:10.1016/j.gr.2022.01.010.

Retallack, G.J., and Landing, E. 2014. Affinities and architecture of Devonian trunks of *Prototaxites loganii*. Mycologia, **106**(6): 1143–1158. doi:10.3852/13-390. PMID: 24990121.

Richardson, J.B., and McGregor, D.C. 1986. Silurian and Devonian spore zones of the old red sandstone continent and adjacent regions. Geol. Surv. Can. Bull. **354**: 1–21. doi:10.4095/120614.

Rubinstein, C.V., and Vajda, V. 2019. Baltica cradle of early land plants? Oldest record of trilete spores and diverse cryptospore assemblages; evidence from Ordovician successions of Sweden. GFF, **141**(3): 181–190. doi:10.1080/11035897.2019.1636860.

Rubinstein, C.V., Vecoli, M., and Astini, R.A. 2011. Biostratigraphy and paleoenvironmental characterization of the Middle Ordovician from the Sierras Subandinas (NW Argentina) based on organic-walled microfossils and sequence stratigraphy. J. South Am. Earth Sci. **31**(1): 124–138. doi:10.1016/j.jsames.2010.07.006.

Schweitzer, H-J. 1983. Die unterdevonfloren des rheinlandes. Palaeontographica, **B189**: 1–138.

Selosse, M.A. 2002. *Prototaxites*: a 400 Myr old giant fossil, a saprophytic holobasidiomycete, or a lichen? Mycol. Res. **106**(6): 642–644. doi:10.1017/S0953756202226313.

Socrates, G. 2001. Infrared and Raman characteristic group frequencies: tables and charts. John Wiley & Sons.

Straka, P., and Sýkorová, I. 2018. Coalification and coal alteration under mild thermal conditions. Int. J. Coal Sci. Technol. **5**(3): 358–373. doi:10.1007/s40789-018-0220-7.

Strullu-Derrien, C., Spencer, ART., Goral, T., Dee, J., Honegger, R. Kenrick, P., et al. 2018. New insights into the evolutionary history of fungi from a 407 Ma Blastocladiomycota fossil showing a complex hyphal thallus. Philos. Trans. R. Soc. B Biol. Sci. **373**(1739): 20160502–20160502. doi:10.1098/rstb.2016.0502.

Strullu-Derrien, C., Wawrzyniak, Z., Goral, T., and Kenrick, P. 2015. . Fungal colonization of the rooting system of the early land plant *Asteroxylon mackiei* from the 407-Myr-old Rhynie chert (Scotland, UK). Bot. J. Linn. Soc. **179**(1): 201–213. doi:10.1111/boj.12307.

Wellman, C.H., Berry, C.M., Davies, N.S., Lindemann, F.-J., Marshall, J.E.A., and Wyatt, A. 2022. Low tropical diversity during the adaptive radiation of early land plants. Nat. Plants, **8**(2): 104–109. doi:10.1038/s41477-021-01067-w. PMID: 35115726.

Wellman, C.H., Steemans, P., and Vecoli, M. 2013. Chapter 29: Palaeophytogeography of Ordovician–Silurian land plants. Geol. Soc. Lond. Mem. **38**(1): 461–476. doi:10.1144/M38.29.

Yafetto, L. 2018. The structure of mycelial cords and rhizomorphs of fungi: a mini-review. Mycosphere, **9**(5): 984–998. doi:10.5943/mycosphere/9/5/3.

Can. J. Microbiol. Downloaded from cdnsciencepub.com by 90.190.215.226 on 05/14/24